Journal of Applied Biology & Biotechnology Vol. 6(06), pp 039-045, November-December, 2018
Available online at http://www.jabonline.in
DOI: 10.7324/JABB.2018.60606

Synergistic Antibacterial Effect of Silver Nanoparticles and Extremely Low-Frequency Pulsed Magnetic Fields on *Klebsiella pneumoniae*

Mai I. El-kaliuoby[1], Alaa M. Khalil[2], Ahmed M. El-Khatib[3], Thanaa I. Shalaby[4]

[1]Physics & Chemistry Department, Faculty of Education, Alexandria University, Alexandria, Egypt.
[2]Basic Sciences Department, Faculty of Engineering, Pharos University in Alexandria, Egypt.
[3]Physics Department, Faculty of Science, Alexandria University, Alexandria, Egypt.
[4]Medical Biophysics Department, Medical Research Institute, Alexandria University, Alexandria, Egypt.

ARTICLE INFO

Article history:
Received on: March 09, 2018
Accepted on: June 01, 2018
Available online: October 20, 2018

Key words: ELF-PMF, AgNPs, *K. pneumonia*, Kinetics of growth, MIC, MBC.

ABSTRACT

The potential use of antibiotics made dramatically increase of antibacterial resistance and the need for different alternatives to antibiotics becomes a must. Recently effects of supplying AgNPs and exposure to ELF-PMF as bactericidal agents were examined alone/and with a combination of antibiotics. This research aimed to explore the synergistic effects of the combination of exposure to ELF-PMF and supplying of AgNPs. *K. pneumonia* bacterium is used as a gram-negative model to be tested undersupplying of different AgNPs concentrations and exposure to ELF-PMF at different frequencies. The best synergistic effect is determined by obtaining a most inhibitory concentration of AgNPs and resonance frequency of ELF-PMF causing maximum inhibition in bacterial growth. Kinetics of growth and MIC/MBC levels showed that exposure to 20 Hz-PMF, 30 min with a supplement of 150 ppm-AgNPs caused a highly synergistic effect by 90% enhancement of growth inhibition. It is concluded that using the benefits of exposure to electromagnetic waves with the presence of nanoparticles can limit the wide-spread of silver nano-products and give a chance of nano-antibacterial agents to be used in safe limits.

1. INTRODUCTION

The wide use of antibiotics in different infections made several types of bacterium to become antibacterial resistant. As a result, production of several multidrug-resistant microbes was generated. *Klebsiella pneumonia* (*K. pneumonia*) is Gram-negative bacteria causes a broad spectrum of diseases, including pneumonia, bacteremia, meningitis and urinary tract infections and has become resistant to many types of antibiotics. At most hospital *k. pneumonia* pathogen infects patients in intensive care units who have got weakened immune systems [1,2,3,4]. Latterly, different research studies were done in multi-directions to find an alternative way for stopping bacterial infections.

Latterly, different research studies were done in multi-directions to find an alternative way for stopping bacterial infections. Using of electromagnetic field (EMF) at an extremely low frequency (ELF) is one of the most recent applications that have great potential to establish different significant interactions to living systems [5-8]. However, the mechanism of interaction and its consequences in living systems is ambiguous and need more work to be clarified. Effects of exposure to ELF-EMF were spotted to be dependent on signal physical characteristics, frequency and field intensity, exposure time and growth stage [9-14]. Several studies were performed to evaluate the bio-effects on bacterium as a result of exposure to such fields and different consequences were approached. Particularly on the bacterial cell, there were remarkable alterations in ultra-structural, changes in growth kinetics, viability reductions, and antibiotic sensitivity, and cellular proliferation, modulations in the flow of ions through membranes and cellular physiological functions as well as cell-to-cell communications [15-23].

Improvement in nanotechnology has opened new skylines in nanomedicine, allowing the synthesis of nanoparticles that could be a powerful weapon against bacteria. Recently, Silver nanoparticles (AgNPs) used as antibacterial agent [24-26] and its effects related to interaction with DNA and RNA, a burst of the cell membrane, interference with cell respiration, and affecting enzyme conformation

*Corresponding Author
Mai I. Elkaliuoby, Physics & Chemistry Department, Faculty of Education, Alexandria University, Alexandria, Egypt.
E-mail: mai.ismail@alexu.edu.eg

[27,28]. On the other hand, many other research studies evoked to prove the potential of integrating AgNPs with antibiotics as a potent antimicrobial key against the bacteria causes resistance to various antibiotics alone [29].

On the same manner, the present work is intended to study the synergistically impact of combination between AgNPs and exposure to ELF as a new method to restrain resistant bacterium.

2. MATERIALS AND METHODS

2.1. Reagents

Silver nitrate ($AgNO_3$, 99.99%), trisodium citrate dehydrate ($C_6H_5O_7Na_3.2H_2O$, 99.99%), and deionized water was purchased from Sigma Aldrich.

2.2. Bacterial Strain

The standard strain of *Klebsiella pneumonia* (*K. pneumonia*) (ATCC 70068) was collected from Global Hospital, Alexandria, Egypt and used for all the current comparative experiments. The bacterial isolates were inoculated on MacConkey agar and incubated at 37°C for 24 h. Bacterial subcultures were produced by suspending three colonies from agar plate into sterilized MacConkey broth media (5 ml for each) and then incubated at 37°C for 24 h. It is worthy to mention that for maintaining a new strain, this step is being done every while before running each experiment.

2.3. Silver Nanoparticles Preparation Method

According to Fang *et al*. (2005) the Silver nanoparticles were synthesized. In brief, 10 mL of $AgNO_3$ solution (5 mM) in deionized water was heated until it began to boil, then 1 mL trisodium citrate solution drops (1%) were added, and continuing of heating until reaching pale yellow color. The solution was cooled to room temperature for further characterizations [30].

3.4 Reaction Mechanism

$$4Ag^{+} + C_6H_5O_7Na_3 + 2H_2O \longrightarrow 4Ag^{0} + C_6H_5O_7H_3 + 3Na^{+} + H^{+} + O_2\uparrow$$

2.5. Characterization of Silver Nanoparticles

Utilizing UV-Vis-spectrophotometer the optical absorption spectrum of Ag colloids was recorded. The morphological shapes and size of silver nanoparticles in Ag colloid were measured with transmission electron microscopy (TEM) operating at 200 kV. The sample was intended by dropping the colloid onto underlying Cu grid tissue paper coated with carbon, leaving behind a film. The FT-IR spectra were obtained by using FT-IR spectrophotometer (Shimazdu IR Prestige-21). The samples were blended uniformly with potassium bromide at 1:100 (sample: KBr) ratio respectively and incubated at 110°C overnight. Then after, the mixture was cooled down in desiccators. A hydraulic press was used for preparing the KBr discs by compressing the powders (a mixture of sample and KBr). The discs were scanned in the range of 400–4000 cm^{-1} to obtain FT-IR spectra.

2.6. Pulsed Magnetic Field Exposure System

The power supply of direct current was used through an electronic switching device to produce an interrupted current of 50% duty cycle with different frequencies. The square-pulsed current (80 mA) then directed to a pair of Helmholtz coils (each of 445 turns and of total resistance 6.8 ohm) separated by a distance 10 cm equal to the radius of the coil to produce a homogeneous magnetic field in form of impulses. The system manufactured at the Electronics physics laboratory in the Faculty of Science, Alexandria University-Egypt. This field measured by using a Gauss/Tesla meter model 4048 at different locations, with probe T-4048.001 (USA) of accuracy ±2% in order to confirm the most homogenous zone (in the midpoint between the two coils) and field intensity found to be (0.32 mT). The tubes (5mL) of bacterial cell suspensions were set in the field point of the coils where PMF was homogeneous. The magnetic field square wave shape was also displayed using the Linear Hall-effect IC sensor on the oscilloscope.

2.7. Bactericidal Test

To examine the bactericidal effect of silver nanoparticles on *K. pneumoniae* bacteria, in approximation 10^5 colony forming units (CFU) of it were inoculated on MacConkey agar plates supplemented with Nano-sized silver particles (AgNPs) in series of concentrations (50, 100, 150, 250, 300, 400, and 500 ppm). The plates were incubated for 24 h at 37°C and the numbers of colonies were counted. For examining the growth rate of bacterial and its growth curve in the supplement of AgNps, bacteria were grown in MacConkey broth medium supplemented with same concentrations of these. Silver-free agar plates cultivated under the same stipulations were used as a control.

To inspect the effect of exposure to PMF on *K. pneumoniae*, samples approximately of 10^5 CFU were cultured in MacConkey broth medium and exposed directly to series of PMF frequencies (0.5, 1, 10, 20, 30, 40 and 50 Hz) for 30 min. Unexposed cultured bacteria under the same stipulations were used as a control. Samples incubated at 37°C and every 1 h the incubations are discontinuous for absorbance measurements and each sample is inoculated on MacConkey agar in order to determine viable cell count. Moreover, the growth inhibition percentage was calculated for all examined samples relative to control one and most inhibitor frequency was determined (resonance frequency).

It is worthy to mention here that all experiments were performed in three replicates and counts corresponding to each particular sample were averaged. Growth kinetics and bacterial growth density were determined by measuring optical density (OD) at 600 nm each 60 min (OD of 0.1 corresponds to a concentration of 10^8 cells per cm^3) [31]. The growth of the inoculums in the broth is indicated by turbidity of the broth and the lowest concentration of the Nano-sized silver particles which inhibited the growth of the bacteria was taken as the minimum inhibitory concentration (MIC) [32]. After specifying MIC level of the AgNPs tested concentrations, an amount of 10 µl from all tubes in which no growth of bacteria was observed inoculated in MacConkey agar plates free of AgNPs. The plates were then incubated for overnight at 37°C. The lowest concentration of antimicrobial agent that kills >99.9% of the initial bacterial population is defined as the Minimal bactericidal concentration (MBC) [33].

Synergistically effect of adding AgNps and exposure to PMF was performed by exposing samples supplemented with different concentrations of AgNPs to the prior determined resonance frequency.

2.8. Statistical Analysis

The statistical analysis was performed using the SPSS for Windows statistical package program (SPSS Inc., ver. 21). All the data are presented as mean ± standard deviation (SD). One-way analysis of variance (ANOVA) was performed to determine the significant

differences between groups. When the one-way ANOVA revealed a significant difference, *post hoc Tukey* test (least significant differences test) was used to determine the differences between specific means. A "*p*" of <0.05 was considered statistically significant and used for all the comparisons.

3. RESULTS

3.1. AgNPs Characterization

3.1.1. TEM Analysis

The typical TEM micrograph of the synthesized AgNPs is presented in Figure 1. The figure depicted that most of the AgNPs were homogeneously distributed and take a spherical shape. Also, it indicated that the particle sizes were ranging from 6.48 nm to 10.7 nm with an average size 8.5 nm.

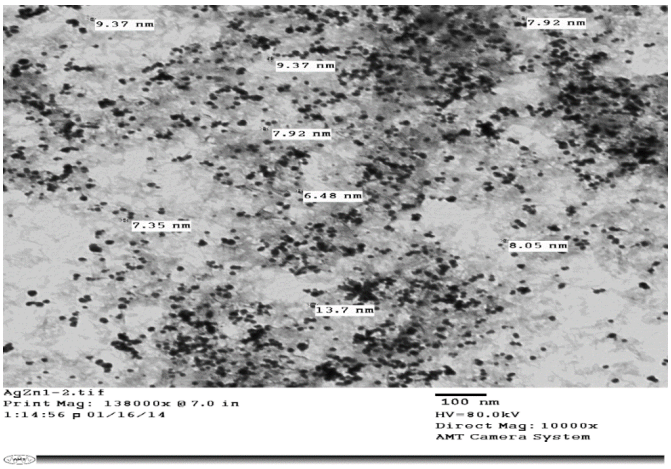

Figure 1: TEM image of AgNPs.

3.2. UV-Visible Spectrum Analysis

UV-Vis spectroscopy is a method that used to examine the production of the nanoparticles based on their optical properties. The UV-Vis analysis of Ag nanoparticles represents the SPR features of Ag nanostructures that are in agreement with those from the previous studies as depicted in Figure 2. The absorption spectrum of Ag nanoparticles (nanosphere) prepared by reduction method shows a sharp SPR feature at 422 nm indicating monodispersity of the sample with no evidence for aggregation [34].

3.3. Fourier-Transform Infrared (FT-IR) Spectroscopy

FTIR spectrum of chemically prepared AgNPs using trisodium citrate showed the absorption band at 2061 cm^{-1} which can be ascribed to citrate precursor –(CH_2) as depicted in Figure 3. The sharp narrow peak at 1648 cm^{-1} corresponds to carbonyl stretching (C=O). The broad O-H peak at 3369-3527 cm^{-1} is due to water molecules appear in the sample.

3.4. Antibacterial Effect of Silver Nanoparticles

Antibacterial effects were performed against *K. pneumonia* bacterium by measuring dynamics of its growth in MacConkey broth media supplemented with different concentrations of AgNPs. The growth characteristics were monitored by taking a reading of O.D. at 600 nm every 1 h after inoculum as shown in Figure 4. The figure depicted that all assigned concentrations of AgNPs caused growth inhibition of *K. pneumonia* and increasing of concentration resulted in more inhibition with maximum effect at 500 ppm of AgNPs.

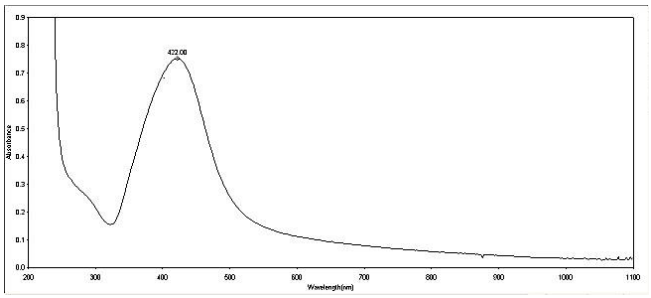

Figure 2: UV-Vis spectra of the Ag nanoparticles.

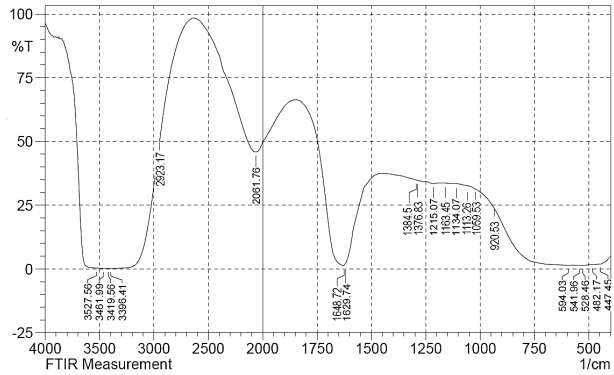

Figure 3: FTIR spectra of the AgNPs chemically prepared by the reduction of silver nitrate with trisodium citrate.

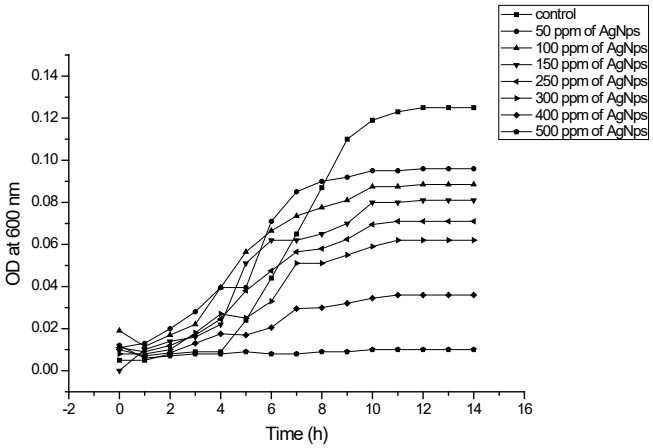

Figure 4: Cell viability growth curves of *K. pneumonia* treated with different concentrations of AgNPs.

3.5. The MIC and MBC

The antibacterial growth inhibition effects were investigated by measuring CFU% grown in MacConkey agar plates inoculated by approximately 10^5 CFU of *K. pneumonia* and supplemented by different concentrations of AgNPs. The MIC and MBC changes due to bacterium counts at each concentration of supplied AgNPs are presented in Figures 5 and 6. The results indicated that MIC level was

to be 400 ppm and MBC was to be 500 ppm that caused more than 90% inhibitions.

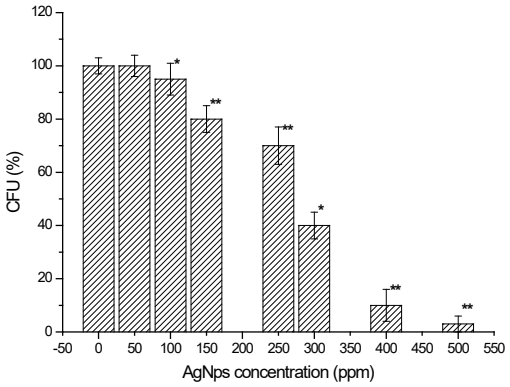

Figure 5: The MIC of AgNPs towards *K. pneumonia*. The data bars represented an average of triplicates CFU% for each AgNPs concentration with STD.
*Statistically significant
**Statistically highly significant

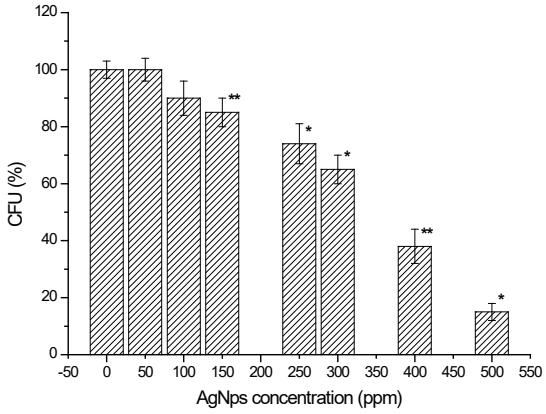

Figure 6: The MBC of AgNPs towards *K. pneumonia*. The data bars represented an average of triplicates CFU% for each AgNPs concentration with STD.
* Statistically significant
** Statistically highly significant

3.6. Antibacterial Resonance Effect of PMF

The characteristics of growth kinetics for *K. pneumonia* under application of PMF at different frequencies are shown in Figure 7. Same dispersions were observed for all assigned exposed samples as compared to unexposed one. It is worthy to indicate that the maximum delay in growth kinetics was obtained after exposure to PMF at a frequency of 20 Hz.

Resonance frequency was determined by applying PMF for 30 min at different frequencies on *K. pneumonia* inoculated in MacConkey broth. The growth inhibition percentages were determined relative to the unexposed ones and resonance curve was performed as shown in Figure 8. The data illuminated highly significant inhibition by 30% for *K. pneumonia* samples exposed to 20 Hz for a period of 30 min.

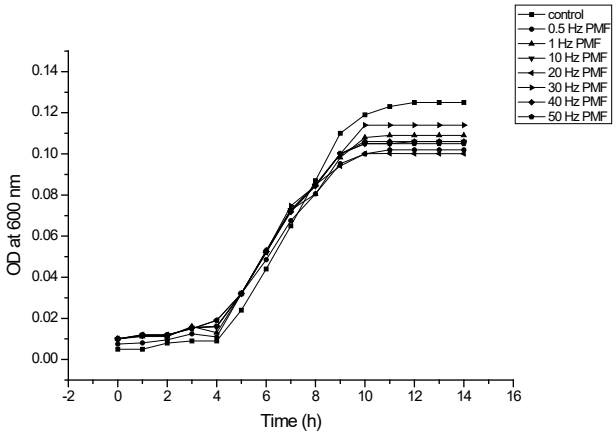

Figure 7: The cell viability growth curves of *K. pneumonia* exposed to different frequencies of PMF.

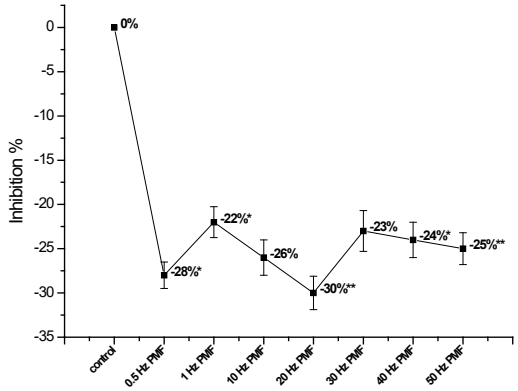

Figure 8: Growth inhibition% with STD of *K. pneumonia* exposed to different frequencies of PMF.
*Statistically significant
**Statistically highly significant

3.7. Synergistic Antibacterial Effect of AgNPs and PMF

Exposure of *K. pneumonia* to the predetermined frequency of PMF with supplementing of AgNPs at different concentrations was performed and curves of growth kinetics were done as shown in Figure 9. The synergistic effects of mixing exposure to 20 Hz and AgNPs at assigned concentrations 50, 150 and 300 ppm were remarkably observed and highly shifted to lower levels. Significant inhibition of growth dynamics by more than 80% was obtained for bacterium supplemented with 300 ppm of AgNPs and exposed to 20 Hz-PMF.

Figure 10 depicts bacterial colonies number that grown on MacConkey plates priory exposed to 20 Hz-PMF, 30 min as a function of AgNPs concentration. The data represented the highly interactive effect of mixing exposure of PMF at the resonance frequency and adding of AgNPs even if it is at low concentration. One may observe that the exposure of PMF with a supplement of AgNPs at a concentration of 150 ppm caused a highly synergistic effect by 90% enhancement of bacterium growth inhibition. On the same manner, no significant growth inhibition was observed for *K. pneumonia* supplied with 300 ppm AgNPs and exposed to 20 Hz-PMF in a way that it acts like supplying of 500 ppm AgNPs alone.

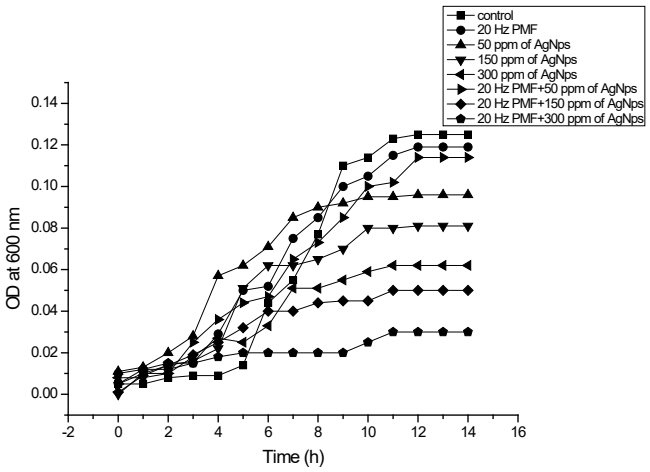

Figure 9: The synergistic effect on *K. pneumonia* of growth curves treated with PMF at different concentrations of AgNPs.

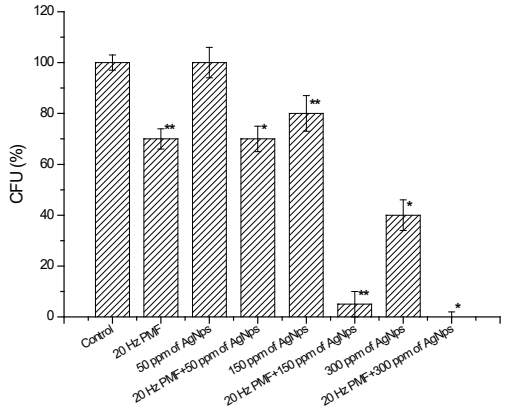

Figure 10: The synergistic effect of treating *K. pneumonia* with PMF (20 Hz) and AgNPs at different concentrations. The data bars represented an average of triplicates CFU% for each AgNPs concentration with STD.
*Statistically significant
**Statistically highly significant

4. DISCUSSION

Antimicrobial resistance is a growing problem in modern healthcare around the world. One of the most common species of bacteria that cause problems in healthcare today is *K. pneumoniae.* Although some treatments still remain, few new ones are being explored, thus the best option is to control the development and spread of antimicrobial resistance [35]. Nanoparticles are yet considered an applicable alternative to antibiotics and appear to have a high potential to solve the problem of the evolution of bacterial multidrug resistance [36]. Among the different nanosized antibacterial agents, AgNPs has proved to be the most effective against a broad spectrum of microbes. This effect particularly is important in the case of Gram-negative bacteria (*K. pneumonia*) as it is able to physically interact with bacterium cell surface [37,38]. In this regards, the kinetics of growth for *K. pneumonia* supplemented with different concentrations of AgNPs were examined and data depicted that all assigned concentrations of AgNPs caused growth inhibition of *K. pneumonia* and increasing of concentration resulted in more inhibition with maximum inhibition at 400 ppm of AgNPs (MIC level). The AgNPs have the ability to be attached to the surface of the cell membrane and cause a disturbance on its permeability and respiration functions [39]. In the same manner, the lowest concentration of AgNPs kills >99.9% of the initial bacterial population where no visible growth of the bacteria (MBC level) was found to be 400 ppm.

The size, shape, and concentration of AgNPs are highly influenced by its bactericidal effects as smaller ones have more ability to penetrate into bacteria [40-42]. The absorption spectrum of synthesized AgNPs indicated monodispersity of the sample with no evidence of aggregation. Also, FTIR spectrum showed absorption band at 2061 cm^{-1} which can be ascribed to citrate precursor –(CH_2). The sharp narrow peak at 1648 cm^{-1} corresponds to carbonyl stretching (C=O). The broad O-H peak at 3369-3527 cm^{-1} is due to water molecules appear in the sample. The results of TEM confirmed that most of the AgNPs has a spherical shape and distributed homogeneously and ranging from 6.48 nm to 10.7 nm.

Our results show resemblance to that smaller dimensions of AgNPs (<30 nm) was found to be most effective against *Staphylococcus aureus* and *K. pneumoniae* [43]. It has a surface/volume ratio much greater than the corresponding bulk material; thus, types and amount of the interactions with the bacterial surfaces are enhanced and determine a higher antibacterial activity.

Exposure to PMF causes a significant delay in growth kinetics and maximum inhibition by 30% was obtained at 20 Hz-PMF which considered as resonance frequency. These findings corroborate with the findings of *Sule et al.* [44] who reported ELF-EMF affects the crucial physicochemical processes in both Gram-positive and Gram-negative bacteria. The exposure effects may cause changes in cell membrane integrity and affect its ionic permeability, which resulted in alterations of ionic concentration and cation uptake capacity of bacterium cell. In the other hand, exposure may modulate the cellular enzymatic activity and rise changes in the spectrum of proteins tightly bound to DNA. As a result of affecting ionic concentration and other enzymes involved in the control of chromatin structure, changes in chromatin conformation were induced and followed by changes in cell growth, DNA and protein synthesis [45-49].

The reaction of mixing exposure to PMF at resonance frequency prior determined and supplying of AgNPs showed highly synergism and significant advanced effects in bacterium growth. Synergistic effect of combining exposure to 20 Hz-PMF and supplying of AgNPs at 300 ppm indicated highly depression in kinetically growth by more than 80%. It is worthy to clarify that supplying of 300 ppm AgNPs combined with exposure to 20 Hz-PMF gave same growth inhibition as supplying of 500 ppm AgNPs alone. Moreover, exposure and supplying of AgNPs at 150 ppm caused a highly synergistic effect by 90% enhancement of bacterium growth inhibition.

5. CONCLUSION

The exposure to PMF increased the ability of AgNPs uptake and hence moved its effect to the higher level of bacterial inhibition. Accordingly, a lower concentration of AgNPs is needed and wide-spread of products containing silver nano-forms will be limited. Moreover, the benefits of electromagnetic waves give chance to safe use of different nano-particles at low permissible concentrations and decrease the possible bio-toxicity.

6. REFERENCES

1. Meatherall B, Gregson D, Ross T, Pitout J, Laupland K. Incidence, risk factors, and outcomes of Klebsiella pneumoniae bacteremia. Am J 2009; 122:866-73.

2. Ko WC, Paterson DL, Sagnimeni AJ, Hansen DS, Von GA, Mohapatra S, *et al*. Community-acquired Klebsiella pneumoniae bacteremia: global differences in clinical patterns. Emerging Infect Dis 2002; 8:160-6.
3. Souli M, Galani I, Antoniadou A, Papadomichelakis E, Poulakou G, Panagea T, *et al*. An outbreak of infection due to beta-Lactamase Klebsiella pneumonia carbapenemase-2 producing *K. pneumoniae* in a Greek university hospital: molecular characterization, epidemiology, and outcomes. Clin Infect Dis 2010; 50:364-73.
4. Elgorriaga IE, Guggiana NP, Dominguez YM, Gonzalez RG, Mella MS, Labarca LJ, *et al*. Prevalence of plasmid-mediated quinolone resistance determinant aac(6′)-Ib-cr among ESBL producing enterobacteria isolates from Chilean hospitals. Enferm Infec Microbiol Clin 2012; 30:466-8.
5. Faqenabi F, Tajbakhsh M, Bernooshi I, Saber-Rezaii M, Tahri F, Parvizi S, Izadkhah M, Hasanzadeh Gorttapeh A, Sedqi H. The effect of magnetic field on growth, development and yield of safflower and its comparison with other treatments. Res J Biol Sci 2009; 4(2):174-178.
6. Martinez E, Carbonell MV, Amaya JM, Maqueda R. Gemination of tomato seeds (Lycopersicon esculentum L.) under magnetic field. Int Agrophys 2009; 23:45-49.
7. Katsenios N, Efthimiadou A, Efthimiadou P, Karkanis A. Pulsed electromagnetic fields effect in oregano rooting and vegetative propagation: A potential new organic method. Acta Agr Scand B-SP 2012; 62(1):94-99.
8. Esitken A, Turan M. Alternating magnetic field effects on yield and plant nutrient element composition of strawberry (Fragaria x ananassa cv. Camarosa). Acta Agr Scand B-SP 2004; 54:135-139. DOI: 10.1080/09064710310019748.
9. Belyaev YI, Alipov YD, Matronchik AY, Radko SP. Cooperativity in E. coli cell response to resonance effect of weak extremely low frequency electromagnetic field. Bioelectrochem Bioenerg 1995; 37:85-90.
10. Belyaev YaI, Alipov YD, Harms-Ringdahl M. Effects of weak ELF on E. coli cells and human lymphocytes: role of genetic, physiological and physical parameters, in: F. Bersani (Ed.), Electricity and Magnetism in Biology and Medicine, Kluwer Academic Publishers, New York, 1999, pp. 481-484.
11. Martirosyan V, Baghdasaryan N, Ayrapetyan S. Bidirectional frequency-dependent effect of extremely low-frequency electromagnetic field on E. coli K-12. Electromagnetic Biology and Medicine 2013; 32(3):291-300.
12. Masoumeh A, Ali-Asghar P, Fatemeh F, Hashemi HJ. Effects of Extremely Low Frequency Electromagnetic Fields On Growth And Viability Of Bacteria. IJRMHS 2013; (1):8-15.
13. Ali FM, Elkhatib AM, Aboutaleb WM, Abdelbacki AM, Khalil AM, El-kaliuoby MI. Control the Activity of Ralstonia Solanacearum Bacteria by Using Pulsed Electric Field. Jokull Journal 2014; 64(4):255-269.
14. Ali FM, Elkhatib AM, Aboutalib WM, Abdelbacki AM, Khalil AM, Serag N. Control of the Activity of Pseudomonas Aeruginosa by Positive Electric Impulses at Resonance Frequency. J Am Sci 2013; 9(10):120-130.
15. Saeed N, Asghar T, Davoud K, Seyyed R, Kaveh E, Khorshid B. Electromagnetic fields on the logarithmic growth of the E. coli. Environ Pharmacol Life Sci 2012; 1(6):26-29.
16. Inhan-Garip A, Burak A, Zafer A, Dilek A, Nilufer O, Tangul S. Effect of extremely low frequency electromagnetic fields on growth rate and morphology of bacteria. Int J Radiat Biol 2011; 87(12):1155-1161.
17. Fojt L, Strasak L, Vetterl V, Smarda J. Comparison of the low-frequency magnetic field effects on bacteria Escherichia coli, Leclercia adecarboxylata and Staphylococcus aureus. Bioelectrochemistry 2004; 63:337-341.
18. Fojt L, Strasak L, Vetterl V. Extremely-low frequency magnetic field effects on sulfate reducing bacteria viability. Electromagn Biol Med 2010; 29:177-185.
19. Gaafar E, Hanafy M, Tohamy E, Ibrahim M. Stimulation and control of E. coli by using an extremely low frequency magnetic field. Romanian J Biophys 2006; 16:283-296.
20. Stange BC, Rowland RE, Rapley BI, Podd JV. ELF magnetic fields increase amino acid uptake into Vicia faba L. roots and alter ion movement across the plasma membrane. Bioelectromagnetics 2002; 23:347-354.
21. Segatore B, Setacci D, Bennato F, Cardigno R, Amicosante G, Iorio R. Evaluations of the effects of extremely low-frequency electromagnetic fields on growth and antibiotic susceptibility of Escherichia coli and Pseudomonas aeruginosa. International Journal of Microbiology, vol. 2012, Article ID 587293, 7 pages, 2012. https://doi.org/10.1155/2012/587293.
22. Fadel M, Wael S, Mostafa R. Effect of 50 Hz, 0.2mT magnetic fields on RBC properties and heart functions of albino rats. Bioelectromagnetics 2003; 24:535-545.
23. Ali FM, Osoris WG, Serag N, Khalil AM. Healing of Guinea Pig Injures Contaminated with Pseudomonas aeruginosa by using 0.7Hz Square Pulsed Magnetic Field (New Method). Int J Curr Res Med Sci 2016; 2(5):6-11.
24. Choi O, Kanjun Deng K, Kim N, Ross L, Surampalli RY, Hu Z. The inhibitory effects of silver nanoparticles, silver ions, and silver chloride colloids on microbial growth. Water Res 2008; 42(12):3066-3074.
25. Babapour A, Yang B, Bahang S, Cao W. Low-temperature sol-gel-derived nanosilver-embedded silane coating as biofilm inhibitor. Nanotechnology 2011; 22(15):155602.
26. Fabrega J, Zhang R, Renshaw JC, Liu WT, Lead JR. Impact of silver nanoparticles on natural marine biofilm bacteria. Chemosphere 2011; 85(6):961-966.
27. Ahamed M, AlSalhi MS, Siddiqui M. Silver nanoparticle applications and human health. Clin Chim Acta 2010; 411(23-24):1841-1848.
28. Shahverdi AR, Fakhimi A, Shahverdi HR, Minaian S. Synthesis and effect of silver nanoparticles on the antibacterial activity of different antibiotics against Staphylococcus aureus and Escherichia coli. Nanomedicine 2007; 3:168-171.
29. Birla SS, Tiwari VV, Gade AK, Ingle AP, Yadav AP, Rai MK. Fabrication of silver nanoparticles by Phoma glomerata and its combined effect against Escherichia coli, Pseudomonas aeruginosa and Staphylococcus aureus. Lett Appl Microbiol 2009; 48:173-179.
30. Fang J, Zhong C, Mu R. The study of deposited silver particulate films by simple method for efficient SERS. Chemical Physics Letters 2005; 401:271-275.
31. Ivan S, Branka S. Silver nanoparticles as antimicrobial agent: a case study on E. coli as a model for Gram-negative bacteria. Journal of Colloid and Interface Science 2004; (275):177-182.
32. Reddy LS, Mary M, Mary J, Shilpa PN. Antimicrobial activity of zinc oxide (ZnO) nanoparticle against Klebsiella pneumonia. Pharm Biol 2014; 52(11):1388-1397.
33. Magana SM, Quintana P, Aguilar DH, Toledo JA, Angeles-Chavez C, Cortes MA, Leon L, Freile-Pelegrin Y, Lopez T, *et al*. Antibacterial activity of montmorillonites modified with silver. J Mol Catal A: Chem 2008; 281:192-199.
34. Mandal S, Selvakannan PR, Pasricha R, Sastry M. Keggin Ions as UV-Switchable Reducing Agents in the Synthesis of Au Core-Ag Shell Nanoparticles. Journal of the American Chemical Society 2003; 125(28):8440-41.
35. Harbarth S, Balkhy H, Goossens H, Jarlier V, Kluytmans J, Laxminarayan R, Pittet D. Antimicrobial resistance: One world, one fight! Antimicrob Resist Infect Control 2015; 4:49. https://doi.org/10.1186/s13756-015-0091-2.
36. Rai MK, Deshmukh SD, Ingle AP, Gade AK. Silver nanoparticles: The powerful nanoweapon against multidrug-resistant bacteria. J Appl Microbiol 2012; 112:841-852.
37. Naraginti S, Sivakumar A. Eco-friendly synthesis of silver and gold nanoparticles with enhanced bactericidal activity and study of silver catalyzed reduction of 4-nitrophenol. Spectrochim Acta A Mol Biomol Spectrosc 2014; 128:357-362.
38. Manjumeena R, Duraibabu D, Sudha J, Kalaichelvan PT. Biogenic

nanosilver incorporated reverse osmosis membrane for antibacterial and antifungal activities against selected pathogenic strains: An enhanced eco-friendly water disinfection approach. J Environ Sci Health A Toxic Hazard Subst Environ Eng 2014; 49:1125-1133.
39. Kvitek L, Panacek A, Soukupova J, Kolar M, Vecerova R, Prucek R, *et al*. Effect of Surfactants and Polymers on Stability and Antibacterial Activity of Silver Nanoparticles (NPs), Journal of Physical Chemistry C 2008; 112(15):5825-5834.
40. Periasamy S, Joo HS, Duong AC, Bach TH, Tan VY, Chatterjee SS, Cheung GY, Otto M. How Staphylococcus aureus biofilms develop their characteristic structure. Proc Natl Acad Sci USA 2012; 109:1281-1286.
41. Rolim JP, de-Melo MA, Guedes SF, Albuquerque-Filho FB, de Souza JR, Nogueira NA, Zanin IC, Rodrigues LK. The antimicrobial activity of photodynamic therapy against Streptococcus mutans using different photosensitizers. J Photochem Photobiol B 2012; 106:40-46.
42. Murtaza H, Ihsan U, Hina Z, Komal N, Arfa I, Huma G, Muhammad A, Nasir M. Biological entities as chemical reactors for synthesis of nanomaterials: Progress, challenges and future perspective; Materials Today Chemistry 2018; 8:13-28.
43. Collins TL, Markus EA, Hassett DJ, Robinson JB. The effect of a cationic porphyrin on Pseudomonas aeruginosa biofilms. Curr Microbiol 2010; 61:411-416.
44. Sule O, Cuce EM, Burak A, Ayse Inhan G. Effect of extremely low frequency electromagnetic fields on bacterial membrane. Int J Radiat Biol 2016; 92(1):42-9.
45. Alipov YD, Belyaev IY, Aizenberg OA, Systemic reaction of Escherichia cells to weak electromagnetic fields of extremely low frequency. Bioelectrochem Bioenerg 1994; 34:5-12.
46. Belyaev IY, Eriksson S, Nygren J, Torudd J, Harms-Ringdahl M. Effects of ethidium bromide on DNA loop organisation in human lymphocytes measured by anomalous viscosity time dependence and single cell gel electrophoresis. Biophys Biochem Acta 1999; 1428:348-356.
47. Heussen C, Nackerdien Z, Smit BJ, Bohm L. Irradiation damage in chromatin isolated from V-79 Chinese hamster lung fibroblasts. Radiat Res 1987; 110:84-94.
48. Belyaev YI, Harms-Ringdahl M. Effects of gamma-rays in the 0.5-50 cGy range on the conformation of chromatin in mammalian cells, Radiat Res 1996; 145:687-693.
49. DelRe B, Bersani F, Agostini C, Mesirca P, Giorgi G. Various effects on transposition activity and survival of Escherichia coli cells due to different ELF-MF signals. Radiat Environ Biophys 2004; 43:265-270.
50. Esitken A, Turan M. Alternating magnetic field effects on yield and plant nutrient element composition of strawberry (Fragaria x ananassa cv. Camarosa). Acta Agr Scand B-SP 2004; 54:135-139.

How to cite this article:
El-kaliuoby MI, Khalil AM, El-Khatib AM, Shalaby TI. Synergistic Antibacterial Effect of Silver Nanoparticles and Extremely Low-Frequency Pulsed Magnetic Fields on *Klebsiella pneumoniae*. J App Biol Biotech. 2018;6(06):039-045. DOI: 10.7324/JABB.2018.60606